

**Jacob Parks**

Mars Dust Adhesion: Characterizing Adhesion Behavior  
of JSC Mars-1 Regolith on Aerogel Substrates

**Faculty Sponsor**

Dr. Firouzeh Sabri



## **Abstract**

The adhesion of dust to critical spacecraft equipment poses a major challenge to planetary exploration. Regolith adhesion can cause issues that drastically reduce the length of missions and threaten the safety of astronauts. Regolith adhesion issues have been reported on both lunar and Mars missions, but Mars presents unique challenges due to triboelectrically charged dust suspended in its atmosphere. Mars regolith adhesion has not been studied extensively on aerogels, despite aerogel's rapidly growing number of space applications. The goal of this research was to understand the characteristics and mechanisms of regolith adhesion onto polyimide and polyurea aerogels under different surface charge conditions with Polydimethylsiloxane (PDMS) as a control. Results show that, in general, there is a strong correlation between higher magnitude surface charge and higher regolith accumulation and coverage.

## Introduction

The adhesion characteristics of planetary regolith create a significant challenge for planetary exploration. Regolith adhesion, which is caused by Van der Waals and electrostatic forces, can cause major issues on spacecrafts [1]. These issues include reduced solar panel efficiency, damage to mechanical equipment, clogged air filters, and covered calibration targets [2]. These challenges have been reported on both Mars and lunar exploration missions [3]. However, Mars presents unique challenges because Mars' atmosphere contains suspended dust, which has been found to collect on spacecrafts at a rate of 0.28% per day [4]. Additionally, Mars experiences planet-wide dust storms which contribute to triboelectric charging of both Mars dust and spacecrafts, increasing adhesion [5].

One area of regolith adhesion research that is lacking is the characteristics of regolith adhesion onto various types of aerogels. Aerogels are a unique class of materials characterized by their extremely low density, porous structure, low thermal conductivity, and high specific surface area [6]. Because of these properties, aerogels are becoming an attractive material for use in space travel and planetary exploration. Aerogels have already been used in cryogenic fluid containment, thermal insulation on the Mars Rover, and high-velocity particle collection on NASA's *Stardust* [7]. Furthermore, new types of shape-memory aerogels could soon be used as self-deployable structures on spacecrafts [8]. Types of polyimide aerogels have also been considered for use as EDL systems, which will become more important as the size of Mars missions' payloads increase [9]. Thus, understanding dust adhesion to these materials can prevent problems when they are further implemented into planetary exploration. The goal of this research is to understand the mechanisms and causes of the adhesion of JSC Mars-1 simulant regolith onto polyurea-crosslinked and polyimide aerogels under various surface charge conditions, with PDMS as a control.

## Experimental Procedures

### Surface Potential Measurements

To understand the impact of electrostatic force on the surface of the materials being tested, surface potential measurements were taken using a Kelvin probe. The Kelvin probe used had a vibrating aperture which was 4.5 mm in diameter and was connected to a Trek Model 325 electrostatic voltmeter. Underneath the probe was a stage that allowed for manual x-y-z motion in increments of 1 mm. The probe was placed 1 mm above the sample as is recommended by the manufacturer to avoid fringe fields. Potential Mea-

surements were taken by raster scanning in increments of 1 mm. From the potential readings, charge was calculated for each point using the equation.

$$Q = U \cdot \frac{\epsilon\epsilon_0 A}{d}$$

where  $Q$  is charge,  $U$  is potential,  $\epsilon$  is the relative electric permittivity of air,  $\epsilon_0$  is the electric permittivity of vacuum,  $A$  is the area of the aperture, and  $d$  is the distance between the probe head and the sample.

### **Regolith Deposition Setup**

Regolith deposition experiments were performed in an inverted set up under atmospheric conditions. Each sample was stored in a desiccator to control exposure to humidity prior to regolith deposition. The samples were sonicated in IPA to remove any dust particles on the surface of each sample. The baseline mass and surface charge of each sample was taken using an analytical balance and Kelvin probe, respectively. Samples were then put under one of three surface charge conditions: baseline, neutralized, or charged. These conditions were achieved by using static neutralizing and charging equipment on each sample. The samples in the neutralized condition were discharged using a Takk Ion-Edge model 400T static eliminator bar. The bar was in a fixed position and samples were placed at a distance of 0.5 cm from the bar, as suggested by the manufacturer. For the samples in the charged conditions, samples were first neutralized, then different amounts of charge were deposited onto their surfaces using a Takk 7081 charging bar. Again, the charging bar was fixed 0.5 cm above samples, as suggested by the manufacturer. After the surface charge conditions were placed on each sample, the samples underwent a controlled exposure to the regolith. Using tweezers, each sample was carefully lowered into a petri dish of JSC Mars-1 simulant regolith. The regolith had been treated in a vacuum oven at 105 °C for several days prior to the experiment to remove as much moisture from it as possible. The samples were removed from the regolith carefully so that only the top surface of each sample was exposed to the dust. The samples were shaken three times to remove any large, loose dust particles. The samples were then massed again and analyzed using optical microscopy.

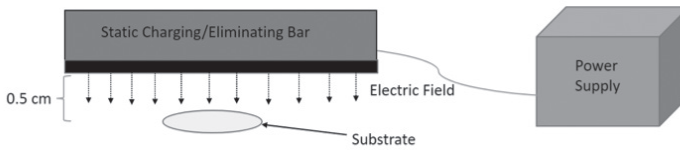


**Figure 1.** Experimental setup for charging/discharging

## ImageJ

The regolith's area coverage on each sample was found from images obtained with a Unitron Examet-5 metallurgical microscope. Percent coverage was calculated through the software ImageJ, which uses thresholding to calculate area coverage. Thresholding is a technique which assigns number values to grayscale images. The software creates a cutoff: any pixel value below the cutoff becomes one category, and any pixel value above the cutoff becomes the other category. The user then must identify which pixel category represents the desired area coverage, and from that percentage the coverage on a substrate can be calculated. Coverage for each substrate was calculated as an average of threshold calculations from several individual images.

## Results And Discussion

### Surface Potential

Baseline surface potential measurements showed a wide range of potential on each substrate. The results of these measurements are shown in Figure 2. Both the polyurea aerogel and the JSC Mars-1 simulant regolith itself were found to have a weak positive surface potential, and, therefore, weak surface charge. Polyimide aerogels and PDMS both exhibited a high magnitude negative surface potential and charge.

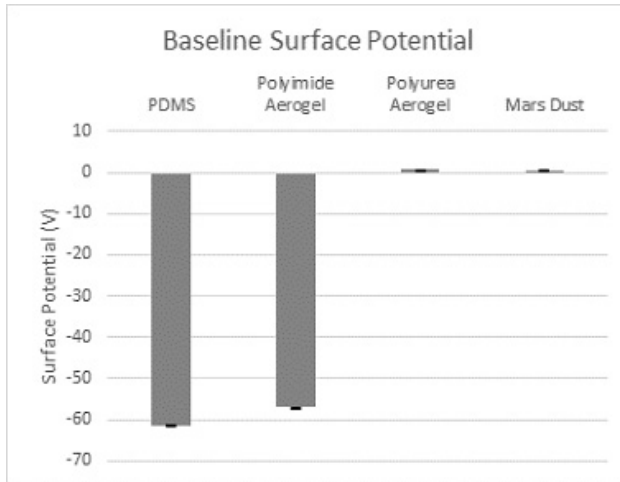
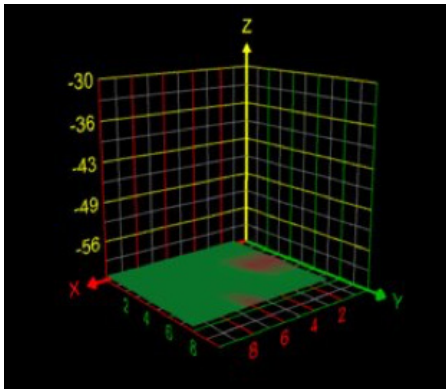
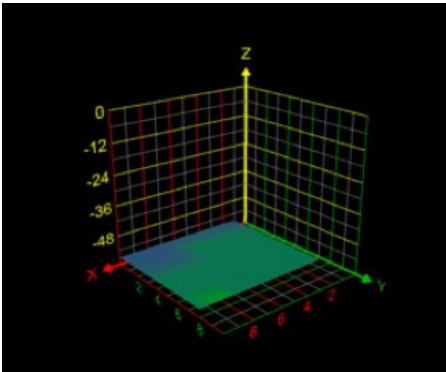


**Figure 2.** Average baseline surface potential for PDMS, polyimide aerogel, polyurea aerogel, and the Mars regolith.

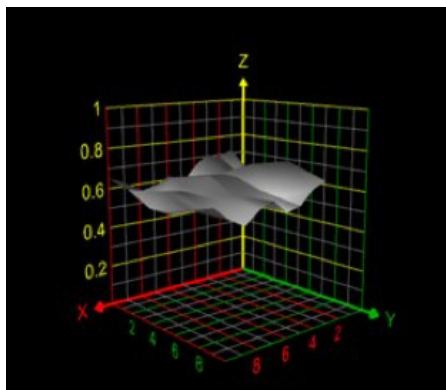
Furthermore, the PDMS and polyimide aerogels exhibited a more uniform potential distribution over the surface, shown in Figures 3a and 3b, respectively. The polyurea aerogel showed a more varied surface potential, with areas of higher and lower relative potential throughout the scanned area, as shown in Figure 3c.



(a)



(b)



(c)

**Figure 3.** Surface Potential Distribution for (a) PDMS (b) polyimide aerogel and (c) polyurea aerogel. The z-axis represents the surface potential in volts.

After electrostatic charging, the change in surface potential after neutralization was found for applied voltages from 1 to 10 kV. Each substrate exhibited similar properties when undergoing changes to surface charge. The samples experienced incrementally higher changes in surface potential with each step of applied voltage until a dielectric limit was reached, as shown in Figure 4. This dielectric limit occurred at 5 kV for PDMS, 6 kV for the polyimide aerogel, and 7kV for the polyurea aerogel. After this limit was reached, no more surface potential could be added to the surface, even with higher applied voltages.

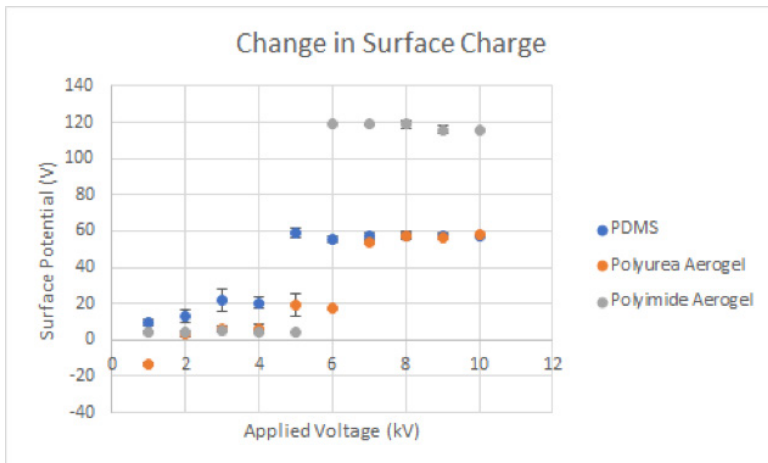


**Figure 4.** Change in surface charge for PDMS, Polyurea aerogels, and polyimide aerogels.

### Gravimetric Analysis

After the dust was deposited onto each substrate using the inverted method, the masses were taken and compared to the baseline for each sample. The results of the gravimetric analysis of the samples at baseline surface charge are shown in Figure 5. At baseline surface charge, PDMS had the highest regolith accumulation, followed by the polyimide aerogel. The polyurea aerogel had the lowest accumulation (Fig. 5). This suggests that the higher the magnitude of surface charge, the higher the regolith accumulation. The regolith accumulation on the samples with 10, 15, and 20 kV of applied potential is also shown in Figure 5. For each sample, except for polyimide aerogel, the regolith accumulation was higher on the charged surfaces than the baseline samples. This is because applying voltage increases the surface potential, thus increasing accumulation.

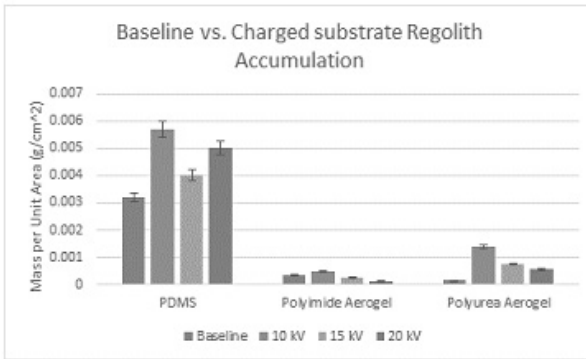


**Figure 5.** Regolith accumulation for each substrate at baseline, 10 kV, 15 kV, and 20 kV.

For each sample, the highest accumulation occurred at 10 kV. This is a direct result of the dielectric limit of each material being below 10 kV. For applied voltages higher than 10 kV, no additional surface potential was being added, so there was no additional regolith accumulation. The results shown in Figure 5 also suggest that the charge of the sample induces an opposite charge on the Mars regolith. Figure 2 shows that at baseline, Mars regolith has a weak positive surface potential. PDMS and polyimide aerogels at baseline have high negative surface potential, while polyurea aerogels have weak positive surface potential at baseline. PDMS and polyimide aerogels both exhibited a change in polarity with high applied voltages. This shows that the Mars regolith can take on both positive and negative charge, because there was adhesion to each substrate regardless of its surface charge polarity. The results of the gravimetric analysis of the neutralized samples are shown in Figure 6. For each neutralized sample, regolith accumulation was lower when compared to the baseline.

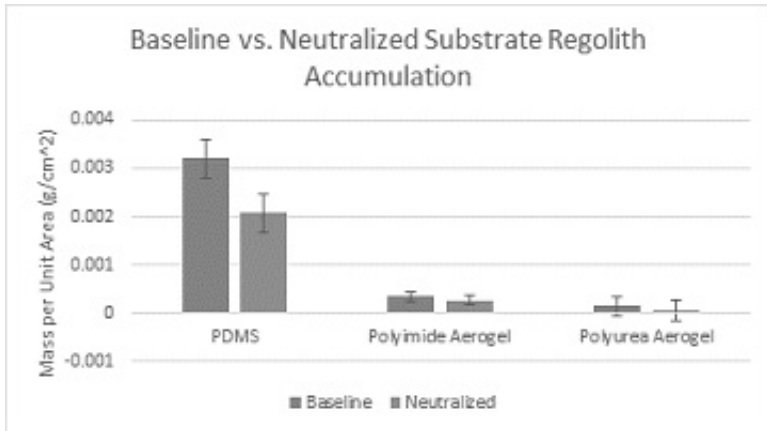


**Figure 6.** Regolith accumulation for each substrate at baseline and after neutralization.

These results again show that higher magnitude surface potential leads to higher regolith accumulation. This also confirms that other factors influence adhesion, because even with the low magnitude surface potential after neutralization, each substrate still accumulated regolith.

### **Optical Microscopy**

The percentage of the substrate area covered by Mars regolith was calculated for each sample using ImageJ software. From this data, a clear relationship between higher surface charge and a higher concentration of dust adhering to the surface of each substrate can be seen. PDMS and polyimide aerogels exhibited the highest and most uniform coverage. The polyurea crosslinked aerogel, which had lower and less uniform charge, exhibited lower and less uniform coverage.

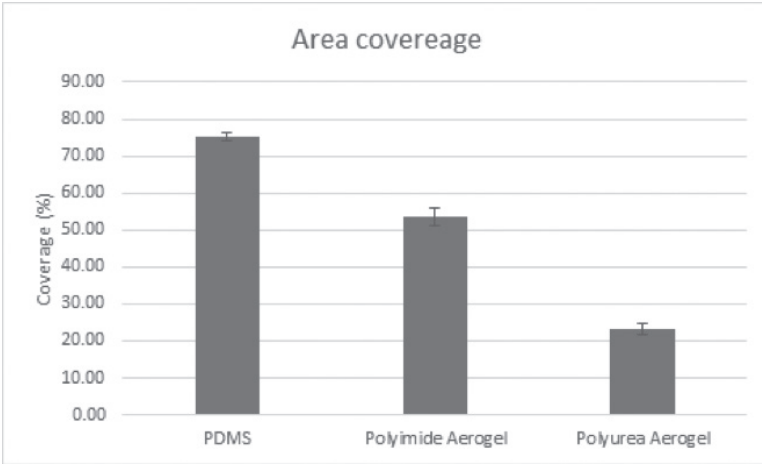


**Figure 7.** Areal coverage for each substrate at baseline surface potential.

The regolith coverage for the other surface potential conditions still needs to be explored. Another observation from optical microscope images was a towering effect which occurred on each substrate. The Mars regolith showed dust-dust adhesion as particles adhered to one another and stacked vertically on the substrate, as described by the schematic in Figure 8. Again, this shows evidence that the polarity of the Martian regolith can be influenced by the surface of the substrate as well as other regolith particles.

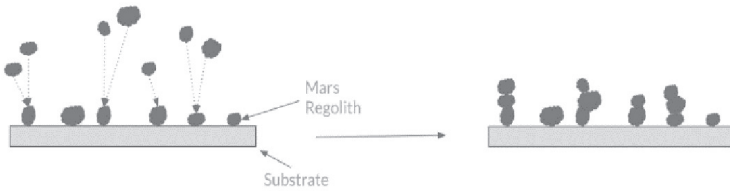


**Figure 8.** Schematic describing the towering effect

## Conclusion

Adhesion characteristics of JSC Mars-1 simulant dust were explored through experimental methods. Experiments were performed on samples with a variety of surface charge conditions under atmospheric conditions in an inverted experimental setup. The effects of surface charge on adhesion behavior was very clear. Higher surface charge on PDMS and polyimide aerogels led to higher area coverage and more regolith adhesion by mass. Lower surface charge, consequently, led to lower coverage and regolith adhesion by mass. When voltage is applied onto the surface of a substrate, a dielectric limit is reached and surface potential no longer increases. This, in turn, keeps regolith adhesion from increasing infinitely as supplied voltage gets higher. Another characteristic of adhesion seen was the towering effect, which shows that there is dust-dust adhesion as well as adhesion between the dust and the substrate itself. This also shows that the samples and other regolith particles can change and induce charge in the Mars Regolith. Further exploration into the effects of low pressure, low humidity, different applied voltages, and temperature will need to be explored using the inverted experimental setup. Surface roughness measurements will also need to be taken before and after dust exposure to explore the relationship between adhesion behavior and surface roughness.

## References

- [1] F. Sabri, T. Werhner, J. Hoskins, A. Schuerger, A. Hobbs, J. Barreto, D. Britt, and R. Duran, *Advances in Space Research* **41**, 118 (2008).
- [2] H. Perko, J. Nelson, and J. Green, *Proceedings of Engineering, Infrastructure, and Sciences*, 1 (2002).
- [3] T. Stubbs, R. Vondrak, and W. Farrell in: *Dust in Planetary Systems*, (NASA, Kauai, HI, 2005, pp. 239-243).
- [4] G. Landis and P. Jenkins, *Journal of Geophysical Research* **105**, 1855 (2000).
- [5] Z. Sternovsky, S. Robertson, A. Sickafoose, J. Colwell, and M. Horanyi, *Journal of Geophysical Research* **107**, 15 (2002).
- [6] A. Pierre and G. Pajonk, *Chem. Rev.* **102**, 4243 (2002).
- [7] S. Jones, *J Sol-Gel Sci Techn* **40**, 351 (2006).
- [8] W. Sokolowski and S. Tan, *Journal of Spacecraft and Rockets*, 1 (2007).
- [9] M. Meador, E. Malow, R. Silva, S. Wright, D. Quade, S. Vivod, H. Guo, J. Guo, and M. Cakmak, *ACS Appl. Mater. Interfaces*, **4(2)**, 536 (2012).